Optics Communications 283 (2010) 4387–4391

Contents lists available at ScienceDirect

Optics Communications

journal homepage: www.elsevier.com/locate/optcom

Optimized design for 2×10^6 ultra-high Q silicon photonic crystal cavities

Zheng Han, Xavier Checoury *, Delphine Néel, Sylvain David, Moustafa El Kurdi, Philippe Boucaud

Institut d'Électronique Fondamentale, Univ Paris Sud, CNRS UMR 8622, Bât. 220, F-91405 Orsay Cedex, France

ARTICLE INFO

Article history:
Received 22 December 2009
Received in revised form 31 May 2010
Accepted 1 June 2010

Keywords:
Photonic
Crystals
Resonators
Waveguides

ABSTRACT

We propose an optimized design for the measurement in transmission of photonic crystal width-modulated line-defect cavities. By controlling the number of holes and rows that separate the cavity from the coupling waveguides, the measured quality factor of the cavity can be tuned to be close to the unloaded one. In the case of a weakly coupled cavity, we measure an ultra-high quality factor that reaches a value of 2×10^6. This value is not obtained for the largest spacing but for an intermediate one. This counter-intuitive result is supported by 3D-FDTD modeling.

1. Introduction

Photonic crystals (PhCs) are attractive for the fabrication of high quality factor and small mode volume cavities opening the route to nonlinear and quantum electrodynamics experiments. Recently, PhC cavities with quality factors near one million and above have been fabricated while their modal volumes remain close to one cubic wavelength [1–5]. However, coupling to such high-Q cavities is a difficult task since a too weak coupling can prevent the measurement while a too strong one can spoil the quality factor. One scheme classically chosen consists in using a PhC waveguide to couple the cavity by side. The quality factor measurement is then made from the top of the cavity with a near-infrared camera [1,4]. If the side waveguide is partly filled with holes, the quality factor can also be measured through the measurement of in-plane transmission [2]. While this scheme is widely used, the coupling, that depends on the number of holes in the waveguide or on the separation of the waveguide and the cavity, must be carefully studied since it can strongly modify the measured Q factor.

In this work, we propose an optimized design for the transmission measurement of weakly coupled photonic crystal width-modulated line-defect cavities with side waveguide filled with holes by controlling the number of holes and separating rows. An ultra-high quality factor value of 2×10^6 is achieved for this type of design. In particular, we show that the largest quality factors are not obtained for the largest separations between the cavity and the access waveguides. The experimental dependence and values of the Q-factor versus the coupling parameters are found in good agreement with those predicted by three-dimensional finite difference in time domain (3D-FDTD) modeling.

2. Description and fabrication of the structures

The studied structures include a PhC cavity, two PhC waveguides to couple to the cavity and two access waveguides suspended by nano-tethers to inject light in the PhC waveguide. Each access waveguide used to inject light in the PhC contains three sections in a manner similar to Ref. [6]. The first section is an inverted taper used to improve the coupling from free space to the suspended single mode waveguide and has some similarities with the one in Ref. [7]. The second section is a single mode waveguide that is suspended with nano-tether in a manner similar to [8]. The third one is a taper that allows an efficient coupling from the single mode waveguide to the PhC waveguide (Fig. 1 top left).

The PhC cavity and the coupling PhC waveguides are very similar to those described in Ref. [2] as seen in Fig. 1 bottom: a cavity is achieved by modulating the width of a basic line defect that initially is $0.98\sqrt{3}a$, where a is the PhC period. The PhC coupling waveguides have a width of $1.02\sqrt{3}a$. In Fig. 1, the separation between the cavity and the coupling waveguide is 5 rows and the number of holes in the coupling waveguide is 25.

The samples were patterned on a SOI wafer with a 200-nm Si layer on a 2-μm oxide layer. The photonic crystal patterns and the suspended access waveguides were designed in a single e-beam lithography step using a 30-kV Raith Elphy writer [9,10]. The PhC holes are insulated using line patterns having a spiral shape starting and finishing at the center of the hole to avoid over-insulating the border of the hole (thick black curve on Fig. 1 top right). This spiral is repeated and rotated 12 times to define the insulation pattern of the whole hole in such a manner that the electronic dose is homogeneously distributed in the hole. Despite the relatively low 20-kV acceleration voltage of the e-beam lithography, such a description of the holes in line mode rather than in surface mode minimizes side effects and leads to very regular hole shapes which are critical to achieve high-Q factor PhC cavities [11]. The

* Corresponding author.
E-mail address: xavier.checoury@ief.u-psud.fr (X. Checoury).

0030-4018/$ – see front matter © 2010 Elsevier B.V. All rights reserved.
doi:10.1016/j.optcom.2010.06.005

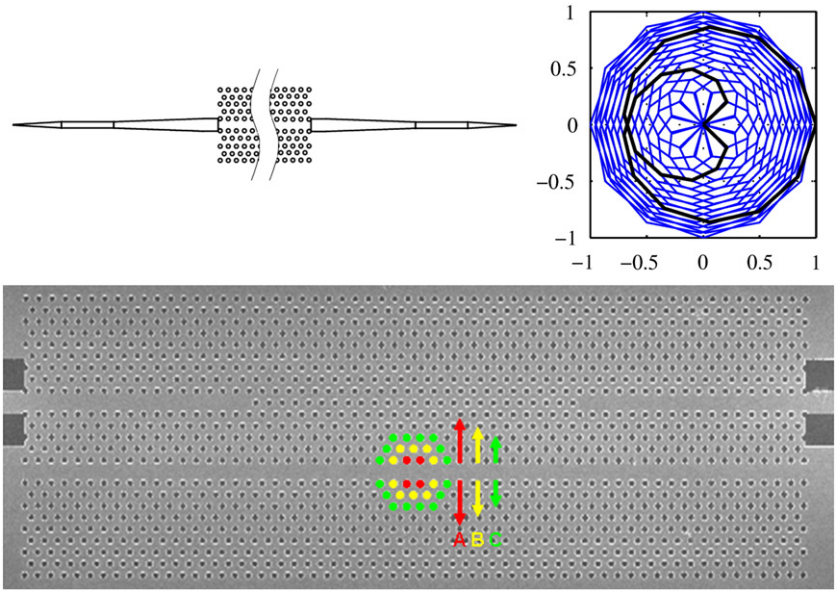

Fig. 1. Top left: schematic view of the whole structure with its access waveguides and tapers. Top right: elementary spiral (thick black curve) and line pattern used for the definition of the holes during e-beam lithography (light blue curve). Bottom: scanning electron microscope (SEM) view of a cavity and the PhC coupling waveguides. The shifted holes of 9 nm, 6 nm and 3 nm are highlighted in red, yellow and green and labeled A, B and C respectively.

holes as well as the strip waveguides were etched through the silicon matrix by inductively coupled reactive ion etching. The samples are then saw diced, with a precision of 2 μm that allows to cut the sample near the taper tip, and wet etched by hydrofluoric acid to remove the underlying silica cladding. The fabricated inverse taper length is 10 μm (Fig. 2 left). Longer tapers are likely to remain stuck on the substrate during the removal of the silica layer. Taper tips of various widths were fabricated and the best coupling with our lensed fiber is achieved with a 270 nm wide tip. The second section of the waveguide is a 450 nm-wide single-mode waveguide suspended by nano-tethers (Fig. 2 right). The length of the tether is 1 μm. Because a distributed feedback (DFB) effect may occur in the access waveguide, the tethers are separated in a non-periodic way by a distance between 30 μm and 34 μm. Rectangular tethers with a width smaller than 100 nm did not provide a satisfying mechanical stability. We thus designed variable width tethers that are 70 nm wide at the side supporting the waveguide and 500 nm at the other side. Butt coupling is an efficient way to couple a strip waveguide to a PhC waveguide [6] and a 60-μm long adiabatic taper allows to match the 450-nm wide access waveguide and the $1.02\sqrt{3}a$ wide, i.e. 742-nm wide, PhC waveguide. The designed photonic crystal waveguides have a length of 25 μm, a lattice period of 420 nm and an air hole radius equal to $0.25a$. The PhC cavities and waveguides are classically fabricated in triangular lattice patterns along the ΓK direction. The displacements of the holes labeled A, B and C that define the cavity are 9 nm, 6 nm and 3 nm respectively. The coupling waveguide has a width of $1.02\sqrt{3}a$ in order to have a good transmission between 1560 nm and 1565 nm where the cavity resonance is expected to occur. The number of rows between the cavity and the coupling waveguide is chosen to be 5 and 6 while the number of holes in the coupling waveguide is varied between 20 and 25. The overall length of the sample is 500 μm to allow an easy handling.

3. Modeling

Using a home-made three-dimensional finite difference in time domain (3D-FDTD) code [12,13], the dependence of the cavity quality factor vs. the coupling strength to the access waveguides is evaluated. As in the experiment, the number of holes in the coupling waveguide is varied between 20 and 25 while the separation between the cavity and the coupling waveguide is 5 and 6 rows. The hole radius r and the Si layer thickness d are equal to $0.25a$ and $0.48a$ respectively where $a = 420$ nm is the lattice constant. The air gap between the membrane and the silicon substrate is 2-μm thick and the silicon refractive index is taken to be 3.45. The FDTD spatial step size is $a/16$.

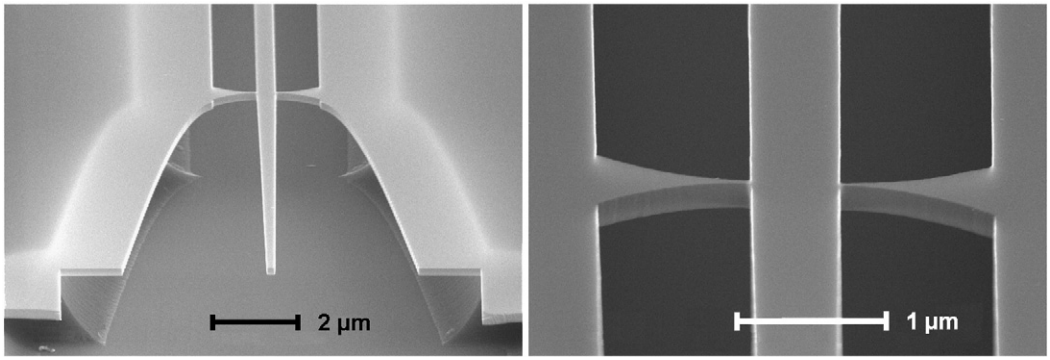

Fig. 2. SEM view of different parts of the suspended waveguide. Left: tilted view of the fiber-to-waveguide inverted taper. Right: tilted view of a tether supporting the access waveguide.

The simulated intrinsic quality factor Q of the cavity, i.e. the cavity without its coupling waveguide in an otherwise unperturbed PhC and without the silicon underlying substrate, is 4×10^7, a value much larger than the experimental ones that have already been achieved [1–4]. However, as seen Fig. 3, when the coupling waveguides as well as the silicon substrate are also considered in the simulation, the quality factor varies from 1.05×10^6 to 6.6×10^6 for 5 rows coupling with 21 to 25 holes and from 1.1×10^6 to 3.3×10^6 for 6 rows coupling with 20 to 24 holes. The quality factor evolves almost linearly with the number of holes in the PhC waveguide and the slope of the curve is larger in the case of five intermediate rows. If the underlying Si substrate is not taken into account, these values are hardly affected. These results clearly show that simulated quality factors are limited by the perturbation of the PhC introduced by the coupling as well as by the coupling losses.

The quality factors of cavities separated from the W1.02 by only five rows can be twice larger than those of cavities with a 6 rows coupling, the quality factor of which being similar to the one reported in Ref. [2]. This is not completely surprising since in Ref. [14], it has been shown that PhC cavities with thin lateral barriers of only a few crystal periods can nonetheless have high quality factors of 1.7×10^6 depending on the external boundary of these barriers. Indeed, in the case of our simulations, the perturbation of the PhC lattice induced by the enlarged W1.02 coupling waveguide may explain this behavior because of a slight modification of the radiation pattern of the cavity.

4. Measurements

Polarization maintaining lensed optical fibers with spot diameter of $\approx$2.75 μm are used to collect and inject light in the access waveguides. The inset of Fig. 4 shows the transmission spectrum of a 480-μm long single mode suspended waveguide alone with two 10-μm long inverted tapers at its extremities. The spectrum is measured with a broad spontaneous emission source and an optical spectrum analyzer (OSA), the resolution of which is set to 0.2 nm. As seen, the total insertion losses, i.e. including lensed fiber connector losses, remain quite low around 13 dB. From the measurement of suspended waveguides of different lengths, the propagation loss has been estimated to be 4 dB/mm. As a consequence, a part of the losses comes from the waveguide with its tethers and the coupling losses are only around 5 dB per taper. The Fabry–Perot fringe contrast remains below 1 dB over a wide bandwidth of 200 nm and indicates that the mode mismatch between the waveguide and the free space is well reduced by the 10-μm long inverted taper. This is an improvement as compared to the 4 dB fringe contrast reported in Ref. [8].

Because we want to measure the quality factor as well as the transmission of PhC cavities, we first characterize the transmission of

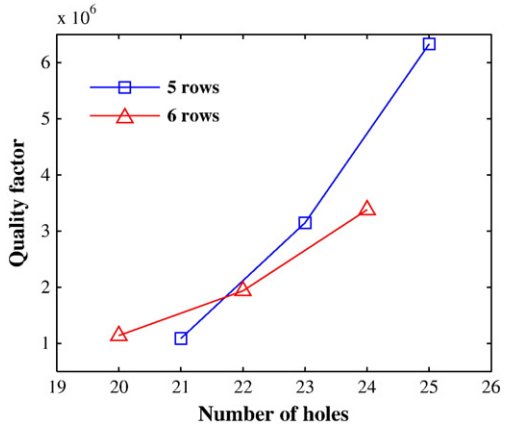

Fig. 3. Simulated quality factor of the loaded cavities as a function of the number of holes in the access waveguide and for two separation distances (3D-FDTD modeling).

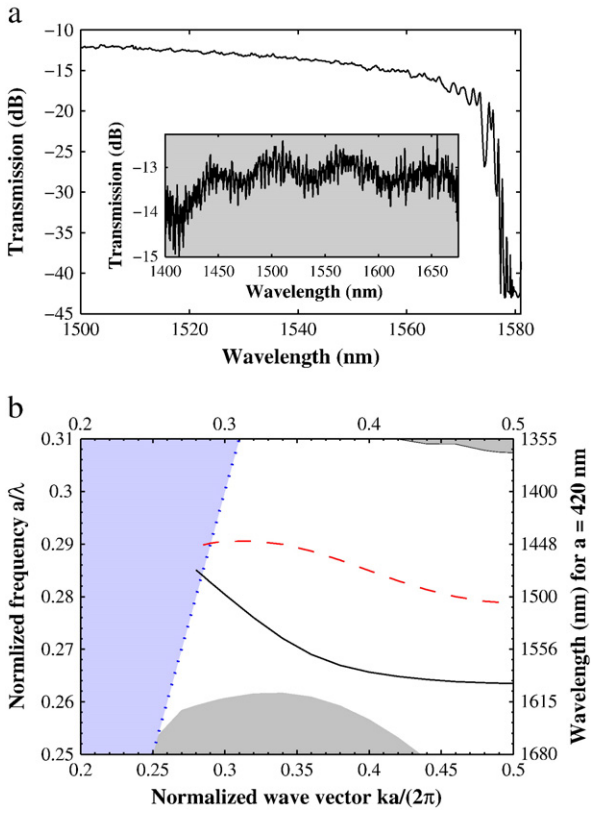

Fig. 4. Top: transmission spectrum of a 25-μm long PhC W1.02 waveguide with its access waveguides (OSA resolution 0.2 nm). Inset: transmission spectrum of a single mode suspended waveguide. The tether width is 70 nm and the length of the sample is 500 μm. Bottom: projected band-diagram of the W1.02 waveguide calculated by a 3D plane-wave method. The light cone is represented by a dotted line. The fundamental mode is represented by a plain line while the first higher order mode is represented by a dashed line.

a W1.02 waveguide alone since it is this waveguide that is used for the coupling to the cavities. Fig. 4 top shows the transmission spectrum of a 25-μm long W1.02 waveguide with its two access suspended waveguides. It comprises two different types of transmission: the first one from 1500 nm to 1570 nm that is almost free from Fabry–Perot resonances and the other one, from 1570 nm to 1580 nm, just before the waveguide cut-off wavelength, consists of Fabry–Perot resonances that are not completely resolved by the spectrum analyzer. As seen on the band diagram of the W1.02 waveguide (Fig. 4 bottom), the first regime corresponds to a frequency range where the group velocity of the light is high in contrast with the second one where the group velocity is low. As expected, in the frequency range of high group velocity, the PhC waveguide and the ridge waveguide have similar mode profiles and group velocities. As a consequence, the W1.02 waveguide is well matched with the access waveguide since the insertion losses of the whole sample are similar to those of the access waveguides alone. The total insertion losses of 13 dB in the frequency range of high group velocity is similar to the one achieved in Ref. [7], and is larger than the 7.9 dB reported in Ref. [6] whereas in this latter case, several lithography steps were required to achieve such a value. The total insertion losses are slightly higher and around 16 dB between 1560 nm and 1565 nm where the cavity resonance is expected to occur. These relatively low total insertion losses will allow to measure the quality factor of weakly coupled cavities. At longer wavelengths, in the low group velocity regime, because of the mode mismatch between the W1.02 and the access waveguide, the W1.02 waveguide behaves like a Fabry–Perot cavity whose resonant modes can be seen. These modes prevent the use of this waveguide at

these wavelengths for the coupling to a cavity since the insertion losses can be higher than 30 dB.

The fabricated cavities are measured by using a tunable laser source with a 0.1-pm resolution. Care is taken to avoid temperature variation of the sample and the injected power in the PhC waveguide is between 10 and 100 nW depending on the transmission of the sample. Fig. 5 top shows the dependence of the quality factor (left) and transmission (right) of six identical cavities as a function of different couplings. The maximum number of holes in the coupling waveguide that allows to achieve a sufficiently high transmitted power for the measurement of the quality factor is 25 and 24 holes in the case of 5 and 6 intermediate rows respectively. As seen, the highest quality factor is around 2 million and is achieved for a cavity 5 rows away from the coupling waveguide in which 25 holes have been drilled. The transmission spectra of cavities coupled to a W1.02 waveguide 5 rows away with 21 and 25 holes inside are represented in Fig. 5 bottom left and right respectively. Because the coupling losses between the fiber and the PhC are low, transmission measurements can be done in the case of very weak cavity couplings and thus almost allow to experimentally get the unloaded Q factor directly. From the transmission measurements and the measured quality factor, the unloaded quality factor of the cavities can be estimated to be between 1.5×10^6 and 2.2×10^6 for the coupling with 5 rows and between 0.99×10^6 and 1.06×10^6 for the coupling with 6 rows. These values are very near from the loaded experimental ones and indicate that the cavities are produced in a very reproducible manner. The rather counter-intuitive fact that a small separation between the cavity and its access waveguide can be more favorable than a larger separation for achieving the highest Q factor, as predicted by the modeling discussed in Section 3, is experimentally observed.

The experimental Q factor is in very good agreement with the simulated one since it is only two to three times lower than the simulated one when coupling waveguides are taken into account. As in the simulations, the quality factor evolves almost linearly with the number of holes in the PhC waveguide and the slope of the curve is larger in the case of five intermediate rows. The lower experimental Q factor is traditionally attributed to fabrication disorder and hole roughness [11]. Indeed, by disturbing the geometry from the ideal map, the symmetry of the lattice gets broken, the scattering is increased and it leads to a reduction of the ideal Q factor. An additional quality factor Q_{loss} can be introduced as in Ref. [15] to take into account these imperfections. The experimental quality factor Q_{exp} is then related to the simulated one Q_{sim} by: $1/Q_{exp}=1/Q_{sim}+1/Q_{loss}$ with a Q_{loss} equal to $\approx3\times10^6$ for a 5-row separation. This value of Q_{loss}, which is related to the accuracy of the current technological processes, limits the achievable Q factors to values near 3×10^6. As a consequence, further increases of the experimental quality factor will require an improvement of technological processes associated with a careful coupling design.

5. Conclusion

In conclusion, we have shown that it is possible to inject light efficiently using a suspended inverted taper and suspended strip waveguides with nano-tethers. The quality factor of PhC cavities has been found dependent on the position of the PhC waveguide used for the coupling. In particular, we have experimentally shown that five intermediate rows lead to larger quality factors than six rows, a situation which is rather counter-intuitive. This has allowed to reach quality factors above 2 million in cavities with a volume of the order of cube wavelength. This work will be useful for further increases of the experimental quality factor since we have shown that a careful design of the coupling is necessary. It will also be helpful for future nonlinear experiments that require the efficient injection of high powers and the collection of very low signals in PhC waveguides and cavities as, for example, in Raman scattering experiments [16,17] since these structures withstand continuous coupled power larger than 100 mW.

Acknowledgments

We thank the Région and C'nano Ile de France for financial support of Zheng Han.

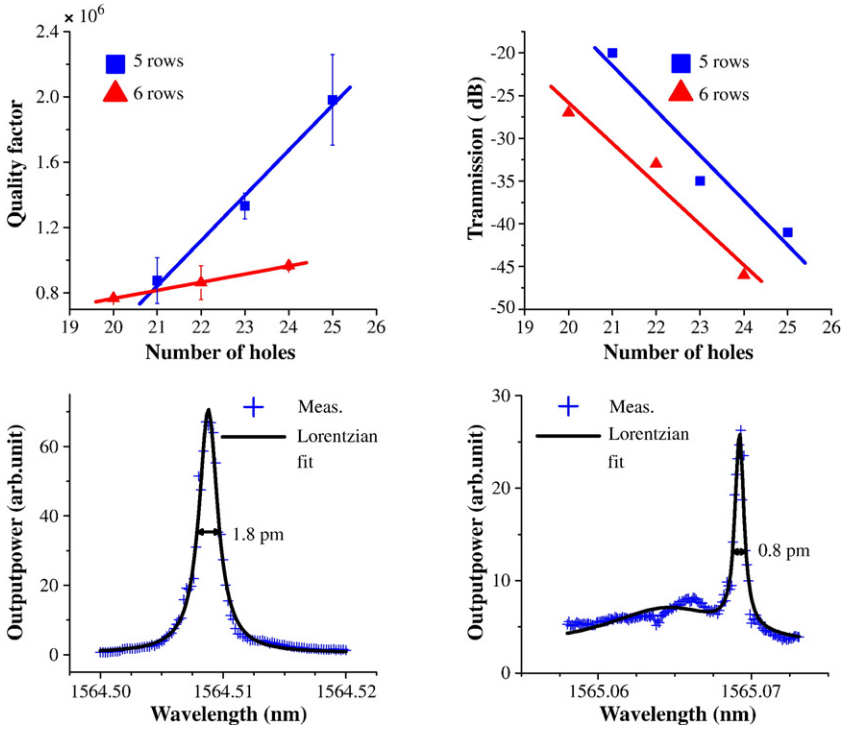

Fig. 5. Top: measured quality factor and transmission. Bottom: measured transmission spectra of the cavity for 21 (left) and 25 (right) holes in a coupling W1.02 waveguide 5 rows away from the cavity. The measured quality factor is above 2 million.

References

[1] B.S. Song, S. Noda, T. Asano, Y. Akahane, Nat. Mater. 4 (3) (2005) 207.
[2] E. Kuramochi, M. Notomi, S. Mitsugi, A. Shinya, T. Tanabe, T. Watanabe, Appl. Phys. Lett. 88 (4) (2006) 041112.
[3] S. Noda, M. Fujita, T. Asano, Nat. Photon. 1 (8) (2007) 449.
[4] S. Combrié, A. De Rossi, Q.V. Tran, H. Benisty, Opt. Lett. 33 (16) (2008) 1908.
[5] Y. Takahashi, Y. Tanaka, H. Hagino, T. Sugiya, Y. Sato, T. Asano, S. Noda, Opt. Express 17 (20) (2009) 18093.
[6] S.J. McNab, N. Moll, Y.A. Vlasov, Opt. Express 11 (22) (2003) 2927.
[7] Q.V. Tran, S. Combrié, P. Colman, A. De Rossi, Appl. Phys. Lett. 95 (6) (2009) 061105.
[8] A. Talneau, K.H. Lee, S. Guilet, I. Sagnes, Appl. Phys. Lett. 92 (6) (2008) 061105.
[9] X. Li, P. Boucaud, X. Checoury, O. Kermarrec, Y. Campidelli, D. Bensahel, J. Appl. Phys. 99 (2) (2006) 023103.
[10] M. El Kurdi, X. Checoury, S. David, T.P. Ngo, N. Zerounian, P. Boucaud, O. Kermarrec, Y. Campidelli, D. Bensahel, Opt. Express 16 (12) (2008) 8780.
[11] H. Hagino, Y. Takahashi, Y. Tanaka, T. Asano, S. Noda, Phys. Rev. B 79 (8) (2009) 085112.
[12] X. Checoury, P. Boucaud, J.M. Lourtioz, O. Gauthier-Lafaye, S. Bonnefont, D. Mulin, J. Valentin, F. Lozes-Dupuy, F. Pommereau, C. Cuisin, E. Derouin, O. Drisse, L. Legouezigou, F. Lelarge, F. Poingt, G.H. Duan, A. Talneau, Appl. Phys. Lett. 86 (15) (2005) 151111.
[13] X. Checoury, S. Enoch, C. Lopez, A. Blanco, Appl. Phys. Lett. 90 (16) (2007) 161131.
[14] E. Kuramochi, H. Taniyama, T. Tanabe, A. Shinya, M. Notomi, Appl. Phys. Lett. 93 (11) (2008) 111112.
[15] Y. Takahashi, Y. Tanaka, H. Hagino, T. Asano, S. Noda, Appl. Phys. Lett. 92 (24) (2008) 241910.
[16] X. Checoury, M. El Kurdi, Z. Han, P. Boucaud, Opt. Express 17 (5) (2009) 3500.
[17] X. Checoury, Z. Han, M. El Kurdi, P. Boucaud, Phys. Rev. A 81 (3) (2010) 033832.